ACS Catalysis

pubs.acs.org/acscatalysis
Research Article

Investigating the Origin of Epimerization Attenuation during Pd-Catalyzed Cross-Coupling Reactions

Isabelle Cai, Thomas C. Malig, Kenji L. Kurita, Joshua S. Derasp, Lauren E. Sirois,* and Jason E. Hein*

Cite This: ACS Catal. 2024, 14, 12331−12341
Read Online

ACCESS | Metrics & More | Article Recommendations | Supporting Information

ABSTRACT: Palladium-catalyzed cross-couplings remain among the most robust methodologies to form carbon−carbon and carbon-heteroatom bonds. In particular, carbon−nitrogen (C−N) couplings (Buchwald−Hartwig aminations) find widespread use in fine chemicals industries. The use of base in these reactions is critical for catalyst activation and proton sequestration. Base selection also plays an important role in process design, as strongly basic conditions can impact sensitive stereocenters and result in erosion of stereochemical purity. Herein we investigate the role of a Pd catalyst in suppressing base-mediated epimerization of a sultam stereocenter during a C−N cross-coupling reaction to access the RORγ inhibitor GDC-0022. Online high-performance liquid chromatography-mass spectrometry (HPLC-MS) was employed to acquire reaction time course profiles and to delineate epimerization behavior, identify decomposition pathways, and monitor Pd-containing species. Our ability to monitor organopalladium complexes in real time by HPLC-MS provided strong evidence that the degree of epimerization was correlated to the Pd speciation in solution. Specifically, Pd(II) complexes were associated with mitigating epimerization of six-membered sultams. Additional studies showed that the suppression of epimerization in the presence of Pd(II) can impact Pd-catalyzed reactions of other substrates such as enolizable ketones, thus providing practical insight on the execution and optimization of such processes.

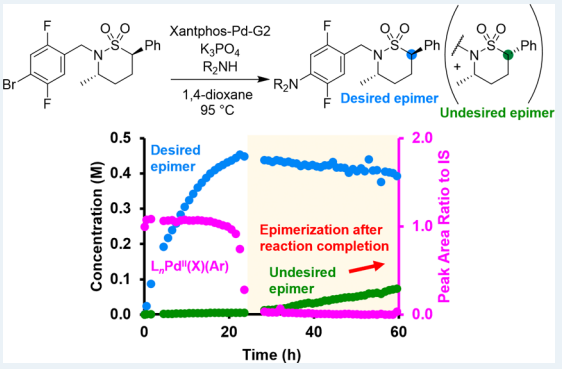

KEYWORDS: *heterogeneous reaction, reaction monitoring, process analytical technology, online HPLC-MS, epimerization, palladium complex, C−N coupling, sultam*

1. INTRODUCTION

Palladium (Pd) catalyzed cross-couplings are a cornerstone of catalysis exemplified by the 2010 Nobel Prize in chemistry and have become prominent in industrial process applications over several decades.[1,2] Consequently, there has been extensive research on the mechanisms of Pd-catalyzed transformations to broaden their applicability and to increase reaction performance while ensuring all critical quality attributes are met.[3−5] In particular, Buchwald−Hartwig aminations used to forge C−N bonds find widespread use in pharmaceutical manufacturing.[6] In-depth reaction analysis and mechanistic studies of such systems, including but not limited to the role and selection of solvent and base,[7,8] are often enabled by process analytical technology (PAT) to collect robust analytical data throughout the reaction's progress.[9,10]

GDC-0022 ((3*S*,6*R*)-**3**) is a cyclic sulfonamide (sultam) active pharmaceutical ingredient (API) which modulates retinoid-related orphan receptor γ (RORγ) and is a candidate for the treatment of immunology-related diseases.[11−13] A key step in its convergent synthesis was a Pd-catalyzed C−N coupling between aryl bromide (3*S*,6*R*)-**2** and triazolo-bicyclic secondary amine **1** (Scheme 1).[14] Pivotal to the success of the cross-coupling was the use of excess of amine **1** (1.2 equiv), Xantphos-Pd-G2 precatalyst (1 mol %),[15] excess potassium phosphate tribasic (K_3PO_4, 1.5 equiv) and potassium acetate (KOAc, 10 mol %).[16] This process was successfully executed on kilogram scale and provided access to GDC-0022 in sufficient quantities for key toxicology studies.[14] Epimerization at the sultam C6 stereocenter in either substrate **2** or product **3**, leading to undesired diastereomer (3*S*,6*S*)-**3**, was a defining challenge of process development for this API. During preliminary reaction optimization, an inverse correlation between precatalyst loading and epimerization was observed. The possibility that the catalyst could attenuate erosion of chiral purity at the sultam C6 stereocenter prompted us to explore this phenomenon and the overall reaction in greater detail, aided by the application of PATs.

Driven by this mechanistic curiosity, herein we report a comprehensive study of the Pd-mediated suppression of sultam

Received: June 10, 2024
Revised: July 24, 2024
Accepted: July 24, 2024
Published: August 3, 2024

Scheme 1. Optimized Conditions of C−N Coupling to Access GDC-0022 ((3*S*,6*R*)-3)

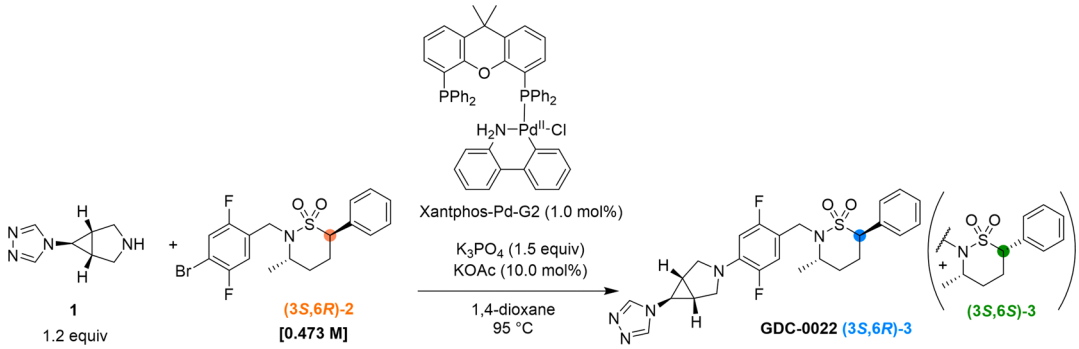

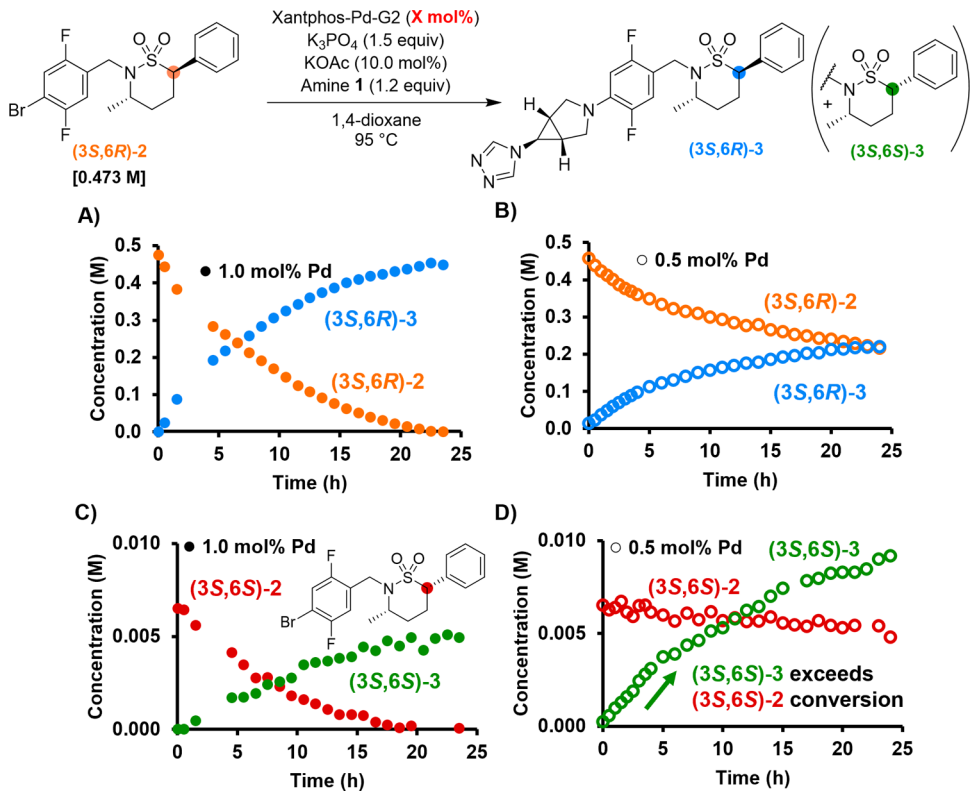

Figure 1. Online HPLC data throughout C−N coupling using different amounts of palladium. (A) Major diastereomer trends using 1.0 mol % [Pd]. (B) Major diastereomer trends using 0.5 mol % [Pd]. (C) Minor diastereomer trends using 1.0 mol % [Pd]. (D) Minor diastereomer trends using 0.5 mol % [Pd]. 1,3,5-trimethoxybenzene (TMB) was employed as an inert internal standard for peak area ratios to account for systematic fluctuations. Conditions: TMB (0.118 M), **1** (0.568 M), (3*S*,6*R*)-**2** (0.473 M), K_3PO_4 (0.710 M), KOAc (0.0473 M), Xantphos-Pd-G2 (0.00473 M/1.0 mol % or 0.00236 M/0.5 mol %), 1,4-dioxane (59 mL).

epimerization using online high-performance liquid chromatography-mass spectrometry (HPLC-MS)[17−22] as the key means to observe the temporal profiles of reaction components. Evidence from this investigation suggested that the presence of a Pd catalyst played a key role in suppressing base-mediated epimerization of the acidic sultam stereocenters. This phenomenon was found to be more broadly applicable by probing the use of different Pd precatalysts as well as different sultam substrates. Notably, the use of online HPLC-MS proved to be a critical feature of this study, enabling acquisition of temporal profiles of different Pd species. Moreover, the potential role of Pd catalysts and related complexes in conserving base-labile stereocenters has direct relevance to systems where such a process is key to reaction success, such as asymmetric α-arylations of ketones.[23−26]

2. RESULTS AND DISCUSSION

2.1. Initial Time Course Analysis of C−N Coupling.

Before beginning our PAT-enabled mechanistic studies, we first reproduced the reported C−N coupling protocol on lab scale. We confirmed excellent conversion and stereochemical purity for the desired (3*S*,6*R*)-**3** product isomer as reported previously. By using 1.0 mol % Xantphos-Pd-G2, we obtained >99% conversion of (3*S*,6*R*)-**2** within 50 h, with a measured dr of 98:2 for the (3*S*,6*R*)-**3** product from a starting dr of 99:1 for (3*S*,6*R*)-**2**. We also confirmed that with 0.5 mol % Xantphos-Pd-G2, the reaction stalled at only 26% conversion after >50 h and formed >10% of the diastereomer (3*S*,6*S*)-**3**. After verifying the performance of the C−N couplings in our laboratories, we set out to adapt our online HPLC-MS system for real-time monitoring of this reaction. Prior work has shown

https://doi.org/10.1021/acscatal.4c03401
ACS Catal. 2024, 14, 12331−12341

that this analytical platform excels in monitoring complex heterogeneous systems and is capable of both chiral and achiral separation.[17] The limited solubility of amine **1** and K_3PO_4 in 1,4-dioxane created logistical challenges regarding accurate sampling and HPLC analysis. To this end, we chose to employ an automated sampling platform leveraging the Mettler-Toledo EasySampler with an EasyFrit attachment. This sampling arrangement allowed the supernatant of the C−N coupling reaction to be sampled selectively.[18] We wanted to expand on this toolkit further by using HPLC-MS to track Pd species to help delineate the role of Pd complexes on any observed epimerization attenuation.[14,20,27]

We repeated the C−N coupling reaction using 1.0 and 0.5 mol % Xantphos-Pd-G2 precatalyst while monitoring the concentration of the diastereomers of aryl bromide **2** and product **3** (Figure 1).[28] The online HPLC data allowed us to track C6 epimerization throughout and after cross-coupling. When using 1.0 mol % [Pd] the profiles of (3*S*,6*R*)-**2** and (3*S*,6*R*)-**3** were mirrored, reaching full conversion within 25 h (Figure 1A). The profiles of (3*S*,6*S*)-**2** and (3*S*,6*S*)-**3** were also mirrored (Figure 1C), thereby correlating conversion of the small amount of diastereomer (3*S*,6*S*)-**2** present at $t = 0$ to the minor epimer of product **3**. The symmetry of trends observed for Figure 1A,C indicated that stereochemical fidelity was being preserved throughout cross-coupling and that epimerization was negligible under these conditions.

Conversely, the reaction time course when using 0.5 mol % Pd precatalyst showed slower conversion and significantly lower overall yield after 25 h (Figure 1B). Moreover, the formation of stereoisomer (3*S*,6*S*)-**3** exceeded what would be expected from the conversion of trace isomer (3*S*,6*S*)-**2** present in the starting material (Figure 1D). These data suggested that epimerization under these conditions was competitive with the desired reaction and provided the first indication that the Pd catalyst concentration was playing a role in suppressing epimerization.

During cross-coupling we observed a Pd species with a m/z ratio matching that of a fragment of the Pd oxidative addition complex of **2**, [Xantphos−Pd−Ar]$^+$ (Figure 2).[14] We also observed that Pd(II) activation to Pd(0), followed by oxidative addition into aryl bromide **2**, seemed to be facile regardless of the amount of Xantphos-Pd-G2 that was charged. When 1.0 mol % Pd precatalyst was used, the [Xantphos−Pd−Ar]$^+$ remained constant for 20 h. This 20-h time point coincides with the time when the starting material (3*S*,6*R*)-**2** was completely consumed (Figures 1A vs 2). In contrast, when 0.5 mol % Pd precatalyst was charged, the [Xantphos−Pd−Ar]$^+$ decreased slowly over 25 h. We attributed this decrease in concentration over time to catalyst deactivation, which also explains the low conversion of (3*S*,6*R*)-**2** (Figures 1B vs 2). Complete reaction profiles of organopalladium complexes collected during cross-couplings are rare, but our online HPLC-MS toolkit proved capable of capturing these trends. We envision that this analytical platform could have broader applications in enabling mechanistic studies that invoke Pd(II) resting states.[29,30]

Having shown a relationship between suppression of epimerization and the amount of precatalyst added, we next wanted to investigate the origin of this phenomenon. It remained unknown whether attenuation of epimerization was primarily due to the metal, the ligand, or both. We began by investigating the effects of the ligand. We hypothesized that if the ligand were responsible for the observed attenuation, this

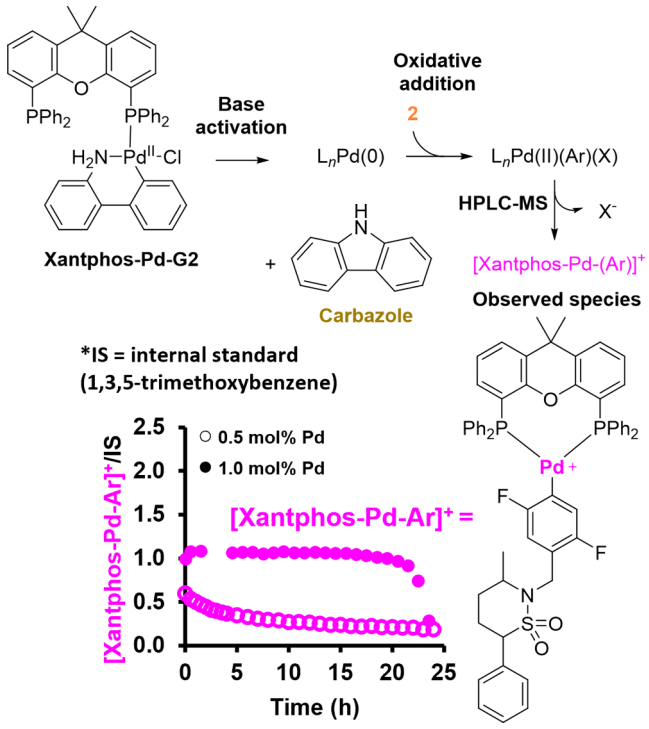

Figure 2. Overlay of observed [Xantphos−Pd−Ar]$^+$ trends from HPLC-DAD. Conditions: TMB (0.118 M), **1** (0.568 M), (3*S*,6*R*)-**2** (0.473 M), K_3PO_4 (0.710 M), KOAc (0.0473 M), Xantphos-Pd-G2 (0.00473 M/1.0 mol % or 0.00236 M/0.5 mol %), 1,4-dioxane (59 mL).

could result from the phosphine acting as a sacrificial reductant. Xantphos oxides formed throughout catalysis could contribute to the epimerization attenuation via consumption of oxidants/base that could promote epimerization.[31−36] Xantphos oxide was indeed detected by HPLC-MS,[14,36] however, tracking the C−N coupling reaction beyond complete conversion showed that significant epimerization of product (3*S*,6*R*)-**3** to (3*S*,6*S*)-**3** only began upon the depletion of the observed [Pd] resting state, [Xantphos−Pd−Ar]$^+$ (Figure 3).[28] This relationship strongly suggested that the suppression of sultam C6 epimerization was related to the presence of a Pd(II) oxidative addition complex. In this case, suppression through irreversible oxidant/base consumption from ligand oxidation or via reaction turnover is unlikely to be active, as overall buffering of the reaction would result in persistent suppression even after depletion of [Xantphos−Pd−Ar]$^+$. This unexpected link between palladium speciation and epimerization exemplifies the utility of collecting time-course data during reaction optimization and execution. In this scenario, unnecessary hold times after reaction completion are not only inefficient from a throughput standpoint, but also contribute to erosion of stereochemical purity.

2.2. Epimerization Control Experiments. To elucidate more nuanced effects of the base on epimerization behavior, we conducted studies using similar sultam substrates with different bases, this time in simplified, noncatalytic systems absent a C−N coupling partner. Consistent with expectations,[37−40] we determined that the epimerization of (3*S*,6*R*)-**2** or its des-bromo analog (3*S*,6*R*)-**4** indeed required base (Table 1, Entry 1 and 7), and furthermore that it was influenced by both the basicity and the solubility of the base. Excess insoluble K_3PO_4 caused epimerization of (3*S*,6*R*)-**2** at high temperature

https://doi.org/10.1021/acscatal.4c03401
ACS Catal. 2024, 14, 12331−12341

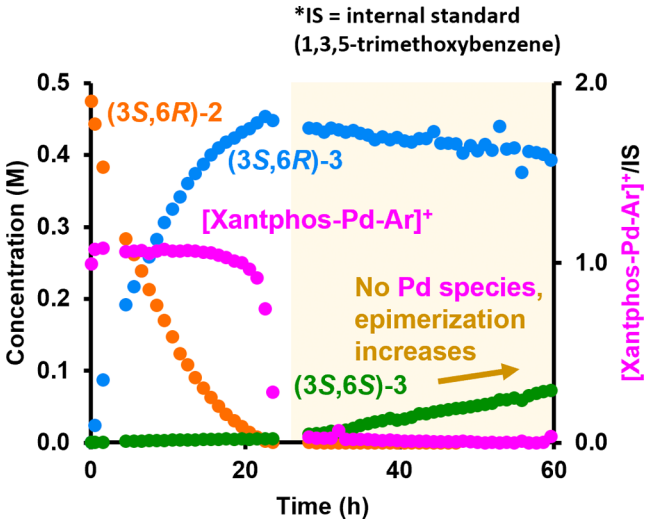

Figure 3. Online HPLC time-course profile during and after cross-coupling. Conditions: TMB (0.118 M), **1** (0.568 M), (3*S*,6*R*)-**2** (0.473 M), K_3PO_4 (0.710 M), KOAc (0.0473 M), Xantphos-Pd-G2 (0.00473 M/1.0 mol %), 1,4-dioxane (59 mL).

Table 1. Epimerization Control Experiments with Different Pd Sources[a]

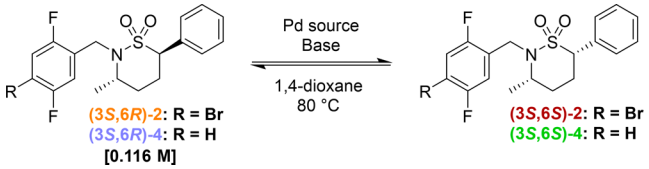

entry	substrate (0.116 M)	base, temperature (°C)	Pd source (5.0 mol %)	dr[b]
1	(3*S*,6*R*)-**2**	none, 80	none	99:1
2		TMSOK (0.01 equiv), 25	none	96:4[c]
3		K_3PO_4 (1.5 equiv), 80	none	95:5
4		K_3PO_4 (1.5 equiv), 80	Xantphos-Pd-G2	99:1
5		K_3PO_4 (1.5 equiv), 80	$Pd(OAc)_2$	99:1
6		K_3PO_4 (1.5 equiv), 80	PEPPSI-IPr	99:1
7	(3*S*,6*R*)-**4**	none, 80	none	99:1
8		K_3PO_4 (1.5 equiv), 80	none	73:27
9		K_3PO_4 (1.5 equiv), 80	$Pd(OAc)_2$	99:1
10		K_3PO_4 (1.5 equiv), 80	$Pd(PPh_3)_4$ (10.0 mol %)	70:30

[a]Expanded timecourse data are available in SI Section S7.2. [b]Sultam dr calculated from HPLC A% at 210 nm, end point taken at 15 h. Initial dr for all experiments shown was 99:1. [c]Sultam dr in Entry 2 was calculated from HPLC A% at 210 nm, end point taken at 1.4 h.

(80 °C), whereas soluble TMSOK resulted in epimerization at room temperature using loadings as low as 1.0 mol % (Table 1, Entry 2 and 3); the similar pK_a's of the conjugate acids of TMSOK and K_3PO_4[41,42] suggested that base solubility therefore played a role in epimerization. The fact that undesired base-mediated epimerization is affected by temperature and solubility of the base suggests that the order of addition of reagents could significantly impact epimerization in such systems. Practically, in cases for which the formation of observed Pd(II) resting state(s)/oxidative addition complex(es) is faster than epimerization, it may be beneficial to have the Pd-catalyst in solution prior to heating the reaction. The relationship between epimerization and solubility of base is also where we began to suspect that sequestration of dissolved K_3PO_4 throughout the C−N coupling contributed to preserving the stereochemical integrity of the sultam substrates.

To further probe whether the relationship between [Pd] and epimerization was specific to Xantphos-Pd-G2, we also studied the epimerization of aryl bromide (3*S*,6*R*)-**2** in 1,4-dioxane at 80 °C in the presence of K_3PO_4 using multiple Pd(II) precatalysts (Table 1, Entries 4−6). A diastereomeric ratio of 99:1 for (3*S*,6*R*)-**2** over the (3*S*,6*S*)-**2** isomer was maintained over 15 h in the presence of Buchwald precatalyst Xantphos-Pd-G2 (Table 1, Entry 4), $Pd(OAc)_2$ (Entry 5), and the *N*-heterocyclic carbene complex PEPPSI-IPr (Entry 6).[43] The effect of Pd(II) was even more pronounced during epimerization studies of des-bromo substrate (3*S*,6*R*)-**4**, which showed >25% epimerization[44] to (3*S*,6*S*)-**4** when heated with K_3PO_4 (Table 1, Entry 8) but negligible formation of (3*S*,6*S*)-**4** when $Pd(OAc)_2$ (5 mol %) was included (Entry 9). These data suggested that suppression of epimerization was not dependent on the identity of the precatalyst.

We carried out additional experiments to probe the epimerization of des-bromo (3*S*,6*R*)-**4** when Pd precatalysts with different oxidation states were added, in order to further deconvolute the influence of Pd(0) versus Pd(II) species. Notably, we used des-bromo substrate **4** as it would not be expected to form the same Pd(II) oxidative addition complex from a Pd(0) source. As illustrated by the reaction time-course data depicted in Figure 4A and further confirmed by end point measurements in Table 1 (Entry 10), $Pd(PPh_3)_4$ (10 mol %) did not slow or reduce the level of epimerization of (3*S*,6*R*)-**4** relative to a control reaction with 1.5 equiv K_3PO_4 in 1,4-dioxane at 80 °C.[45] In stark contrast, suppression of epimerization was clearly observed over 15 h in the presence of 5 mol % $Pd(OAc)_2$ (Figure 4B). These results demonstrated that the oxidation state of palladium was playing a key role in the epimerization attenuation, and led us to consider two remaining hypotheses to account for our observations: (1) Pd(II) mediates a diastereoselective protonation of the sultam C6 carbanion;[46] (2) sequestration of dissolved base by Pd(II) attenuates epimerization.

2.3. Identifying the Role of Palladium throughout Epimerization Attenuation. We began testing our two remaining hypotheses by assessing the impact of Pd oxidative addition complexes on an equilibrated mixture of product diastereomers. Under basic conditions, if Pd(II) were able to mediate diastereoselective kinetic protonation of the sultam C6 anion (Hypothesis 1), one would expect that introduction of the Pd catalyst and/or a Pd(II) oxidative addition complex would shift the mixture back toward diastereomeric purity. To test this hypothesis, we carried out an experiment where we dosed Xantphos-Pd-G2 and 1-bromo-4-fluorobenzene (ArBr) to a 75:25 mixture of (3*S*,6*R*)-**3** and (3*S*,6*S*)-**3**, pre-equilibrated for 15 h at 80 °C in the presence of K_3PO_4 (Figure 5). The combination of the Pd-precatalyst and the aryl bromide allowed us to form a [Xantphos−Pd−Ph]$^+$ complex in situ, as observed by HPLC-MS. After the addition of this Pd(II) source, we observed minimal change in the diastereomeric ratio over the next 25 h. The outcome of this experiment suggests that Pd(II) is not competent at shifting

https://doi.org/10.1021/acscatal.4c03401
ACS Catal. 2024, 14, 12331−12341

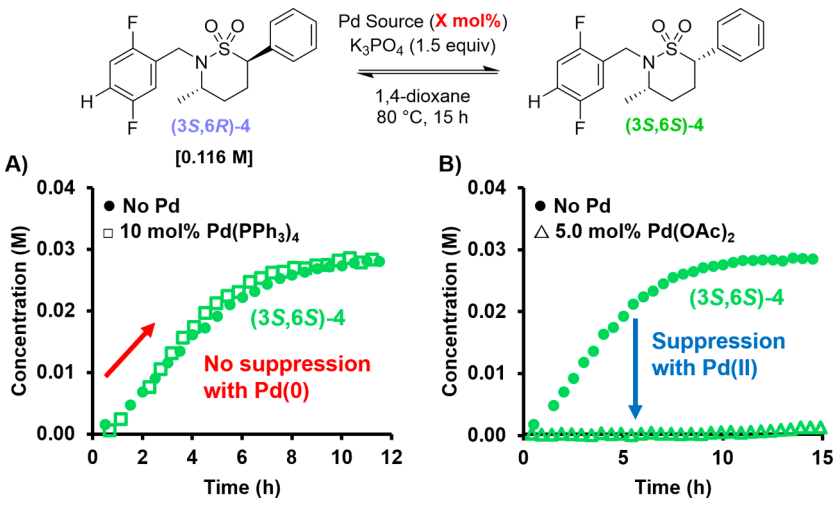

Figure 4. Effects of Pd source on epimerization, comparing Table 1, Entry 9 vs 10. (A) With and without $Pd(PPh_3)_4$. (B) With and without $Pd(OAc)_2$. Conditions: (3*S*,6*R*)-**4** (0.116 M), Pd source (none, $Pd(OAc)_2$ at 0.0058 M/5 mol %, or $Pd(PPh_3)_4$ at 0.0116 M/10 mol %), K_3PO_4 (0.174 M), TMB (0.029 M), 1,4-dioxane (12 mL), 80 °C.

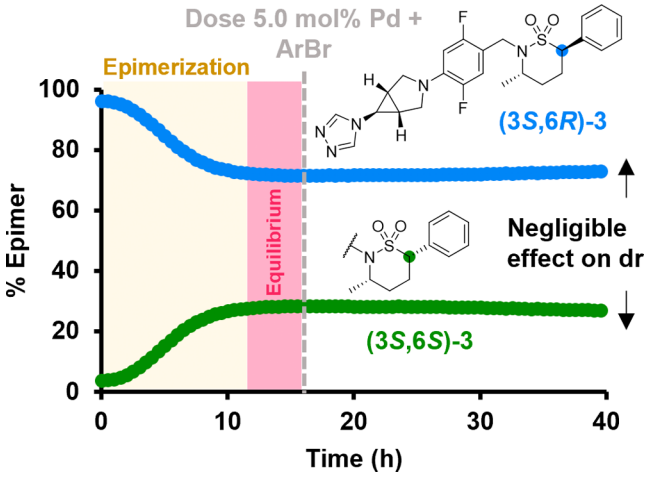

Figure 5. Testing validity of Hypothesis 1 via a Pd(II) dosing experiment. Conditions: (3*S*,6*R*)-**3** (0.116 M), K_3PO_4 (0.174 M), TMB (0.029 M), Xantphos-Pd-G2 (0.0058 M/5 mol %), 1-bromo-4-fluorobenzene/ArBr (0.116 M), 1,4-dioxane (12 mL), 80 °C. Expanded timecourse data are available in **SI** Section S7.3.

the diastereomeric ratio of the epimers following equilibration in the presence of base, and that Hypothesis 1 is not operative.

To better understand any deprotonation/protonation events at the sultam C6 stereocenter, we conducted deuterium incorporation experiments.[47] We expected two possible outcomes from this type of experiment, the first scenario being that significant deuterium incorporation at C6 would be observed in all sultam diastereomers. This would suggest that epimerization suppression is independent of deprotonation/protonation events. In another scenario, suppression of base-mediated deprotonation would be supported by a lack of deuterium incorporation at the C6 stereocenter in sultam isomers.

The C−N coupling reaction was repeated in the presence of D_2O (1.0 equiv). Online HPLC-MS was used to track both the reaction's progress (Figure 6A) and relative ion abundance (Figure 6B). The time-course data collected over 60 h showed two distinct regions of reactivity. The first regime lasted 18 h and showed formation of (3*S*,6*R*)-**3** throughout cross coupling. The second regime, from 18 h onward, showed erosion of the stereochemical purity of (3*S*,6*R*)-**3** via C6 epimerization. Consistent with Figure 3, the transition between the two reactivity regimes corresponded to the time where depletion of the catalyst resting state ($[Xantphos-Pd-Ar]^+$ complex) was observed.

We monitored the $[M + H + 1]^+$ mass signals of key reaction components to measure deuterium uptake throughout both regimes. We initially observed conflicting data, wherein deuterium appeared to incorporate in both diastereomers of the product **3** but not in the aryl bromide substrate **2**. However, characterization of the isolated product (3*S*,6*R*)-**3** with ^1H NMR spectroscopy eventually revealed that deuterium incorporation was occurring at the triazole moiety and not at the sultam stereocenters. This unexpected site of deuterium incorporation likely resulted from Pd-catalyzed heteroaryl C−H activation, which is not uncommon among triazole substrates.[48] A lack of deuterium incorporation at the epimerizable C6 center after reaction completion was likely due to complete consumption of D_2O via this competitive triazole C−H activation pathway as well. Overall, the results of these deuterium incorporation experiments suggested that suppression of sultam epimerization arose from mitigation of deprotonation at C6, although deuterium uptake at the triazole was confounding and required additional experiments.

To further explore Hypothesis 2, we next performed deuterium uptake experiments to probe the effects of added Pd(II) on deprotonation at C6 using des-bromo substrate (3*S*,6*R*)-**4**. The lack of triazole on (3*S*,6*R*)-**4** increased the likelihood that deuterium uptake would occur at C6 of the sultam. We selected $Pd(OAc)_2$ as our Pd(II) source and used D_2O as the deuterium source. A stark difference in the amount of deuterium uptake between the two conditions was observed (Figure 7). More than double the amount of deuterium uptake at C6 was observed for both isomers of **4** when no Pd(II) was added. These data further demonstrated the apparent effect of Pd(II) on modulating proton transfer at the C6 stereocenter of these sultam substrates.

Although Hypothesis 2 was supported by our deuterium incorporation experiments, it was unclear how catalytic Pd(II) could attenuate epimerization in the presence of a large excess

https://doi.org/10.1021/acscatal.4c03401
ACS Catal. 2024, 14, 12331−12341

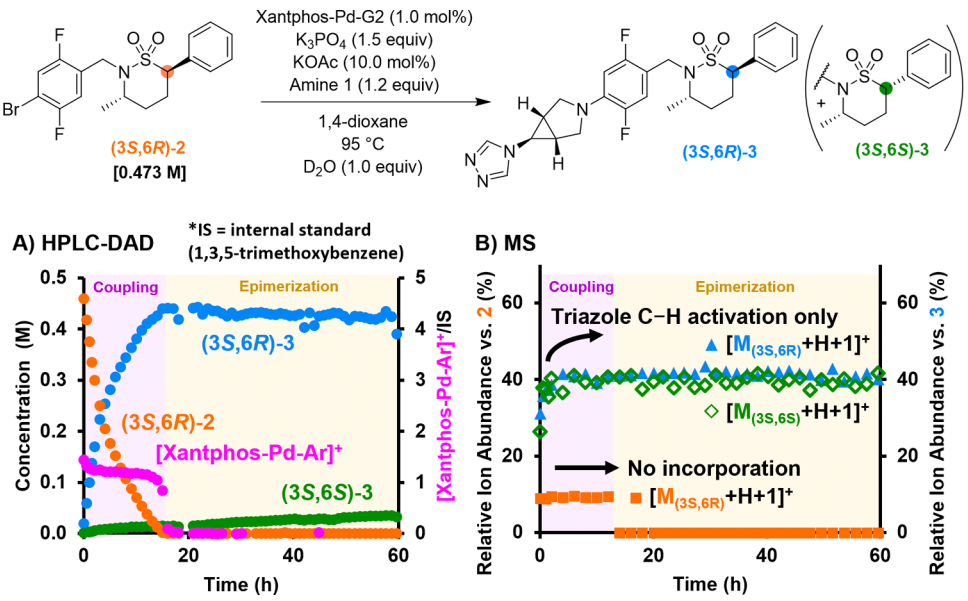

Figure 6. Reaction profiles of deuterium incorporation experiments. (A) HPLC-DAD reaction profiles. (B) Real-time ESI-MS data. Conditions: TMB (0.118 M), **1** (0.568 M), (3*S*,6*R*)-**2** (0.473 M), K_3PO_4 (0.710 M), KOAc (0.0473 M), Xantphos-Pd-G2 (0.00473 M/1 mol %), D_2O (0.118 M).

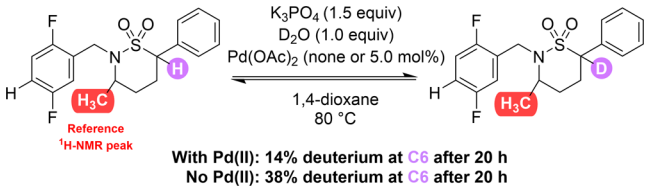

Figure 7. Results of end point deuterium incorporation experiments using (3*S*,6*R*)-**4**. Conditions: (3*S*,6*R*)-**4** (0.116 M), K_3PO_4 (0.174 M), $Pd(OAc)_2$ (none or 5.0 mol %/0.0058 M), 1,4-dioxane (2.0 mL), D_2O (0.116 M), 80 °C, 20 h. Further details are available in **SI** Section S7.4.

of base. We hypothesized that the limited solubility of K_3PO_4 in 1,4-dioxane could enable catalytic amounts of Pd(II) to coordinate most of the solubilized base.[49] However, in these systems, K_3PO_4 is always saturated; Pd-coordination of phosphate would continuously facilitate dissolution of more phosphate, eventually resulting in a greater concentration of dissolved base than palladium. It is possible that the dissolution of K_3PO_4 is slow enough such that Pd(II) can coordinate the amount dissolved during the reaction.

An alternative hypothesis may be that trace amounts of KOH (present in the K_3PO_4 source or formed from residual water in the reaction milieu) are responsible for the epimerization, and that attenuation of epimerization proceeds via sequestration of KOH by Pd(II) to form Pd–OH complexes. The formation of Pd–OH complexes is well-known, and they may exist alongside or as part of Pd-oxidative addition complexes.[50] The amount of KOH present in this system is expected to be low, as the reaction was performed using dry solvents under an inert atmosphere. Moreover, the pK_a of K_2HPO_4 (12.4)[41] relative to that of water (15.7) suggests an equilibrium strongly favoring the tribasic phosphate. Taken together, we hypothesize that the concentration of KOH in situ remains lower than that of the catalyst, enabling Pd(II) species to act as a sink for KOH and to suppress epimerization through the formation of Pd(II)–OH. This hypothesis is also in line with the dependence of suppression on Pd-loading, as well as the lack of suppression observed with Pd(0) species.

Figure 8 illustrates our proposal for Pd-mediated epimerization suppression as part of the general catalytic cycle of a typical Buchwald–Hartwig amination.[6] Steps I–IV in the catalytic cycle involving intermediates **i**–**iii** are conventional mechanistic steps in a Buchwald–Hartwig amination. We propose in off-cycle Steps V–VI that KOH mediates the epimerization of our sultam diastereomers, and epimerization suppression predominantly occurs due to ligand exchange of Pd oxidative addition complex **i** with KOH to form the Pd–OH complex **iv**.

As we hypothesized that the main source of epimerization was the trace amount of water and the subsequent action of any KOH formed, we sought to confirm the effects of the addition of water to the system. When water (10 mol %) was added during the epimerization of (3*S*,6*R*)-**2** in the presence of K_3PO_4, we indeed observed an overall increase in epimerization over 15 h relative to the baseline control reaction (Figure 9; for further details see SI Section S8.2). We also observed that epimerization started to attenuate with much higher doses of water, however, this may be the result of water changing the bulk properties of the reaction solution and phosphate speciation and could still be consistent with our hypothesis.

Given these partly confounding data, we decided to probe this effect further via the portionwise addition of TMSOK as a soluble base, with online monitoring to determine the point at which epimerization begins. Earlier experiments revealed that a 1.0 mol % charge of TMSOK (relative to substrate) partially epimerized (3*S*,6*R*)-**2** (Table 1, Entry 2). If Hypothesis 2 were operative, epimerization suppression should depend on the ratio of TMSOK to [Pd(II)]. We tested this relationship by sequentially charging TMSOK into a solution of (3*S*,6*R*)-**2** to trigger epimerization (Figure 10). The results clearly demonstrated that TMSOK could be dosed until a breaking point in suppression was observed at greater than twice the amount of $Pd(OAc)_2$ (with the precatalyst charged at 10 mol % relative to substrate). These data further confirmed that

https://doi.org/10.1021/acscatal.4c03401
ACS Catal. 2024, 14, 12331–12341

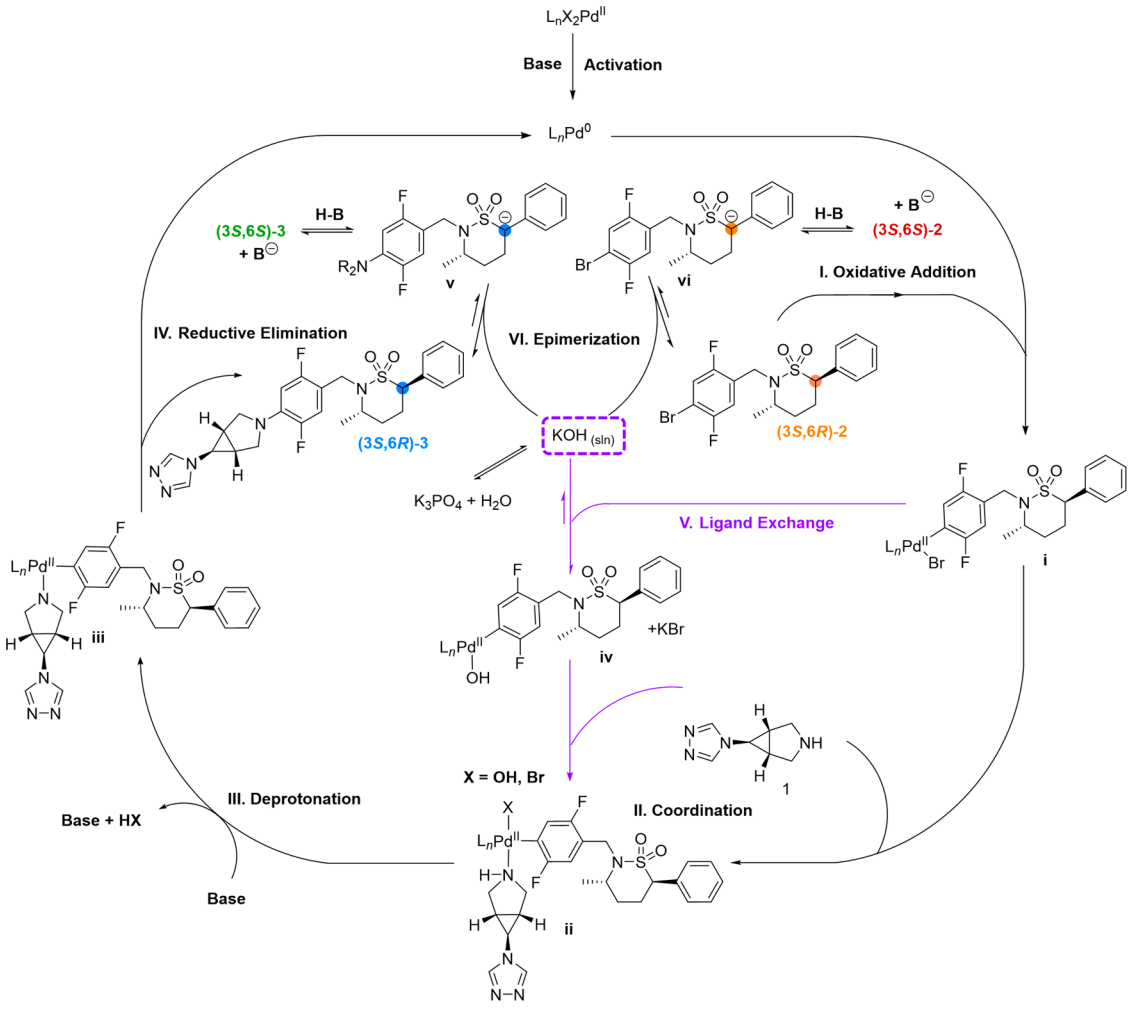

Figure 8. Proposed catalytic pathway for the C−N coupling and sequestration of base by Pd(II).

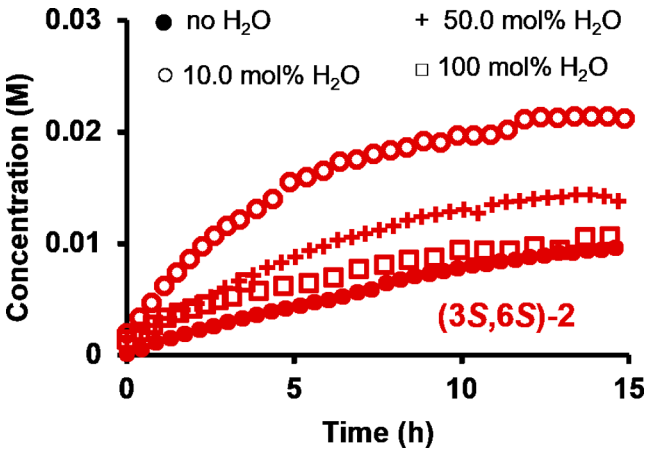

Figure 9. Epimerization control experiments with added water. Conditions: (3*S*,6*R*)-**2** (0.116 M), K_3PO_4 (0.174 M), TMB (0.029 M), H_2O (0, 0.0116, 0.058, or 0.116 M), 1,4-dioxane (12 mL), 80 °C. Further details and expanded timecourse data are available in SI Section S7.5.

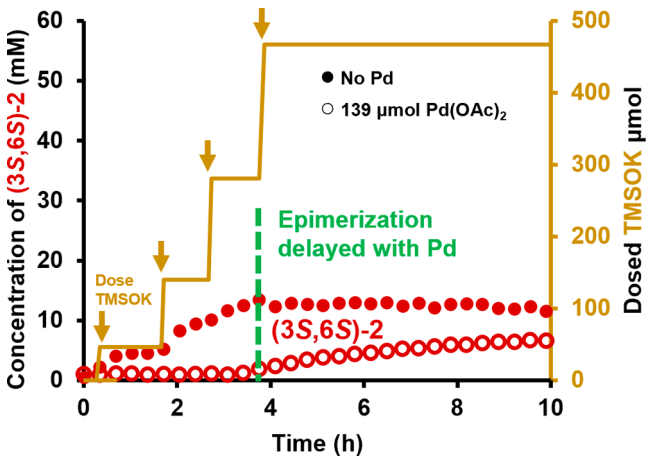

Figure 10. TMSOK dosing experiment. Conditions: (3*S*,6*R*)-**2** (0.116 M), K_3PO_4 (0.174 M), TMB (0.029 M), $Pd(OAc)_2$ (0 or 0.0116 M/10 mol %), TMSOK (0.0935 M in 1,4-dioxane, doses: 0.5, 1.0, 1.5, 2.0 mL), 1,4-dioxane (12 mL), 25 °C. Expanded timecourse data are available in SI Section S7.6.

some degree of epimerization could be triggered by substoichiometric amounts of a soluble base, analogous to the effects of trace amounts of KOH in solution, and that an appropriate amount of Pd(II) offered a protective effect against epimerization up to the likely point of saturating the metal species.

2.4. Further Exploration of Other Substrates. With a better understanding of the nature of this sultam epimerization

https://doi.org/10.1021/acscatal.4c03401
ACS Catal. 2024, 14, 12331−12341

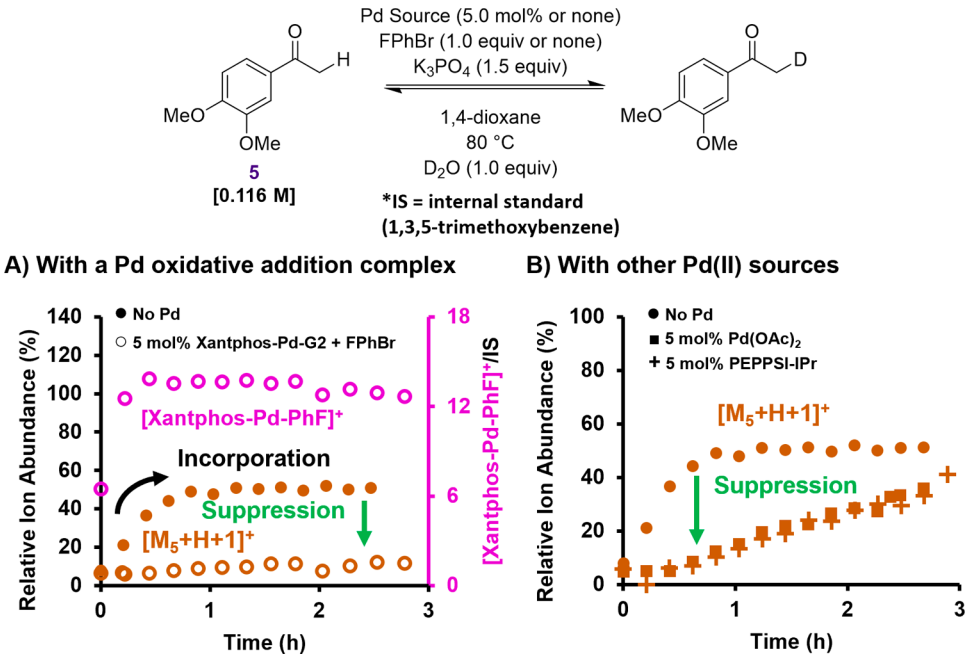

Figure 11. Reaction profile data of deuterium incorporation in **5**. (A) Real-time ESI-MS data of $[M + H + 1]^+$ ion of **5** and HPLC-DAD data of L_n–Pd–Ar species over time. (B) Real-time ESI-MS data of $[M + H + 1]^+$ of **5** with other Pd sources. Conditions: 5 (0.116 M), Pd source (none or 5.0 mol %/0.0058 M), 1-bromo-4-fluorobenzene (0.116 M or none), K_3PO_4 (0.174 M), 1,4-dioxane (12 mL), D_2O (0.116 M), 80 °C. Note: Due to the presence of an aryl bromide, α-arylation of 5 was observed at later time points during the reaction performed in (A). For more details see SI Section S7.7.

attenuation phenomenon, we sought to probe its generality to other Pd-catalyzed systems. To preserve the stereochemistry of enantioenriched substrates throughout Pd catalysis, reactions are often performed using mild conditions[51−53] or by using tailored substrates.[54−56] Based on our findings, we suspected that other cases existed in which the Pd-catalyst could be playing a role in conserving stereochemical integrity, potentially even unbeknownst to the chemist. Among many others, a representative system in which this behavior might manifest could be the Pd-catalyzed acylative cross-coupling of acid chlorides with enantioenriched benzyltrifluoroborates to synthesize α-aryl acetophenones.[57] This reaction demonstrated unique stereospecificity for inversion of the chiral center during transmetalation, and the stereochemistry of the relatively acidic α-stereocenter in the product was well-retained despite conditions including excess base at high temperature and minimal steric constraints.[57]

Inspired by this example and using acetophenone **5** as a simple mass-active model substrate estimated to have a similar pK_a to the sultam substrates (pK_a ∼ 24),[58,59] we carried out deuterium incorporation experiments to examine if added Pd(II) could modulate deuterium uptake in the presence of K_3PO_4 in 1,4-dioxane. To better track the lifetime of Pd(II) in solution, we used a combination of Xantphos-Pd-G2 and 1-bromo-4-fluorobenzene to generate a L_nPd(Ar)(X) species in situ, which we could observe by HPLC-MS. As illustrated in Figure 11A, the results of the experiment suggested that the presence of a Pd(II) oxidative addition species substantially suppressed deuterium incorporation into acetophenone **5**.

This effect was also evident for the presence of $Pd(OAc)_2$ and PEPPSI-IPr.[37] While the final amount of deuterium incorporation was the same, the rates of incorporation with and without a Pd(II) species diverged sharply, demonstrating the suppression effect of different Pd sources (Figure 11B). Additional experiments revealed that epimerization suppression was also dependent on the pK_a of the targeted substrates (see SI Table S5). These results again demonstrated the importance of PAT data in reaction optimization and process development, as time-course analysis can allow for the detection of phenomena otherwise difficult to catch with reaction end point analysis alone. Given the use of anhydrous conditions with inorganic bases in some of the most common palladium catalyzed cross-couplings (Suzuki–Miyaura or Heck reactions, Buchwald–Hartwig aminations, C–H activation), we believe this work has widespread implications across the field of Pd-catalyzed couplings.[5,57,60,61]

3. CONCLUSIONS

In summary, we have reported a study of the Pd-associated suppression of sultam C6 epimerization in heterogeneous reaction systems employing K_3PO_4, using online HPLC-MS to monitor these processes in real time. The ability to detect Pd complexes throughout the reaction time course allowed us to determine that Pd(II) was required for suppression to occur. The comparative lack of deuterium incorporation at C6 of sultam substrates in the presence of D_2O during the C–N coupling suggested that there was no proton transfer at the stereocenter while Pd(II) was present in solution. Furthermore, deuterium control experiments enabled us to confirm that this Pd-mediated phenomenon was not specific to sultams. Based on these results, we proposed that Pd(II) could modulate basic activity in solution via coordination of hydroxide, thereby suppressing epimerization at acidic/enolizable centers. These insights, enabled by PAT, likely hold significance for the process development of similar Pd-catalyzed heterogeneous cross-coupling reactions involving substrates with base-labile stereocenters.

https://doi.org/10.1021/acscatal.4c03401
ACS Catal. 2024, 14, 12331−12341

■ ASSOCIATED CONTENT

Supporting Information

The Supporting Information is available free of charge at https://pubs.acs.org/doi/10.1021/acscatal.4c03401.

Experimental procedures, expanded experimental data, additional experiments, and characterization (PDF)

■ AUTHOR INFORMATION

Corresponding Authors

Lauren E. Sirois − *Department of Synthetic Molecule Process Chemistry, Genentech, Inc., South San Francisco, California 94080, United States;* orcid.org/0000-0002-1948-3749; Email: sirois.lauren@gene.com

Jason E. Hein − *Department of Chemistry, The University of British Columbia, Vancouver, British Columbia V6T 1Z1, Canada; Department of Chemistry, University of Bergen, Bergen N-5020, Norway; Acceleration Consortium, The University of Toronto, Toronto, Ontario M5G 1X6, Canada;* orcid.org/0000-0002-4345-3005; Email: jhein@chem.ubc.ca

Authors

Isabelle Cai − *Department of Chemistry, The University of British Columbia, Vancouver, British Columbia V6T 1Z1, Canada*

Thomas C. Malig − *Department of Synthetic Molecule Analytical Chemistry, Genentech, Inc., South San Francisco, California 94080, United States;* orcid.org/0000-0003-3168-2297

Kenji L. Kurita − *Department of Synthetic Molecule Analytical Chemistry, Genentech, Inc., South San Francisco, California 94080, United States*

Joshua S. Derasp − *Department of Chemistry, The University of British Columbia, Vancouver, British Columbia V6T 1Z1, Canada*

Complete contact information is available at: https://pubs.acs.org/10.1021/acscatal.4c03401

Author Contributions

L.E.S., T.C.M., K.L.K., and J.E.H. conceptualized the project. I.C. carried out experimental work. L.E.S., T.C.M., K.L.K., J.S.D., and J.E.H. supervised the research, K.L.K. also carried out HRMS analysis for elucidation of sultam decomposition. K.L.K. and T.C.M. also helped isolate minor stereoisomers. All authors participated in data analysis and discussed the results. All authors contributed to preparing the manuscript and Supporting Information.

Funding

Financial support for this work was provided by the Canada Foundation for Innovation (CFI-35833), Genentech, Inc., Natural Sciences and Engineering Research Council of Canada (RGPIN-2021−03168, Discovery Accelerator), and the University of British Columbia. This research was undertaken thanks in part to funding provided to the University of Toronto's Acceleration Consortium from the Canada First Research Excellence Fund (CFREF-2022−00042). Student support was provided by an NSERC CGS-M scholarship and UBC's 4YF scholarship (IC).

Notes

The authors declare no competing financial interest.

■ ACKNOWLEDGMENTS

The authors thank Genentech, Inc., for their donation of key compounds and gratefully acknowledge Mettler-Toledo Autochem for their generous donation of process analytical equipment (EasyMax, EasySampler, and EasyFrit) to JEH. The authors also thank Dr. Andrew J. Kukor and Dr. Tristan Maschmeyer (formerly of Hein Lab), and Sara Guzman, Arcadia Lau, and Paloma Prieto (Hein Lab) for assistance with data visualization. We also acknowledge David Lao (formerly of Genentech, Inc.) for preliminary studies of the C−N coupling reactions of (3*S*,6*R*)-**2**, and Dr. Janis Jermaks (Genentech, Inc.) for computational predictions of substrate pK_a values.

■ ABBREVIATIONS

API: active pharmaceutical ingredient
dr: diastereomeric ratio
HPLC: high performance liquid chromatography
HPLC-MS: high performance liquid chromatography − mass spectrometry
HPLC-DAD: high performance liquid chromatography − diode array detector
NMR: nuclear magnetic resonance
MS: mass spectrometry
PAT: process analytical technology
Pd: palladium
PEPPSI-IPr: pyridine-enhanced precatalyst preparation stabilization and initiation − isopropyl
RORγ: retinoid-related orphan receptor γ
TMB: 1,3,5-trimethoxybenzene
TMSOK: potassium trimethylsilanoate
UV/vis: ultraviolet/visible spectroscopy

■ REFERENCES

(1) Seechurn, C. C. C. J.; Kitching, M. O.; Colacot, T. J.; Snieckus, V. Palladium-Catalyzed Cross-Coupling: A Historical Contextual Perspective to the 2010 Nobel Prize. *Angew. Chem., Int. Ed.* **2012**, *51*, 5062−5085.

(2) Torborg, C.; Beller, M. Recent Applications of Palladium-Catalyzed Coupling Reactions in the Pharmaceutical, Agrochemical, and Fine Chemical Industries. *Adv. Synth. Catal.* **2009**, *351*, 3027−3043.

(3) Farina, V. How to Develop Organometallic Catalytic Reactions in the Pharmaceutical Industry. *Org. Process Res. Dev.* **2023**, *27*, 831−846.

(4) Devendar, P.; Qu, R. Y.; Kang, W. M.; He, B.; Yang, G. F. Palladium-Catalyzed Cross-Coupling Reactions: A Powerful Tool for the Synthesis of Agrochemicals. *J. Agric. Food Chem.* **2018**, *66*, 8914−8934.

(5) Ruiz-Castillo, P.; Buchwald, S. L. Applications of Palladium-Catalyzed C−N Cross-Coupling Reactions. *Chem. Rev.* **2016**, *116*, 12564−12649.

(6) Forero-Cortés, P. A.; Haydl, A. M. The 25th Anniversary of the Buchwald−Hartwig Amination: Development, Applications, and Outlook. *Org. Process Res. Dev.* **2019**, *23*, 1478−1483.

(7) Sunesson, Y.; Limé, E.; Lill, S. O. N.; Meadows, R. E.; Norrby, P. Role of the Base in Buchwald−Hartwig Amination. *J. Org. Chem.* **2014**, *79*, 11961−11969.

(8) Dennis, J. M.; White, N. A.; Liu, R. Y.; Buchwald, S. L. Pd-Catalyzed C−N Coupling Reactions Facilitated by Organic Bases: Mechanistic Investigation Leads to Enhanced Reactivity in the Arylation of Weakly Binding Amines. *ACS Catal.* **2019**, *9*, 3822−3830.

(9) Mathew, J. S.; Klussmann, M.; Iwamura, H.; Valera, F.; Futran, A.; Emanuelsson, E. A. C.; Blackmond, D. G. Investigations of Pd-

Catalyzed ArX Coupling Reactions Informed by Reaction Progress Kinetic Analysis. *J. Org. Chem.* **2006**, *71*, 4711−4722.
(10) Murray, J. I.; Zhang, L.; Simon, A.; Elipe, M. V. S.; Wei, C. S.; Caille, S.; Parsons, A. T. Kinetic and Mechanistic Investigations to Enable a Key Suzuki Coupling for Sotorasib Manufacture—What a Difference a Base Makes. *Org. Process Res. Dev.* **2023**, *27*, 198−205.
(11) Cyr, P.; Bronner, S. M.; Crawford, J. J. Recent Progress on Nuclear Receptor RORγ Modulators. *Bioorg. Med. Chem. Lett.* **2016**, *26*, 4387−4393.
(12) Pandya, V. B.; Kumar, S.; Sachchidanand; Sharma, R.; Desai, R. C. Combating Autoimmune Diseases with Retinoic Acid Receptor-Related Orphan Receptor-γ (RORγ or RORc) Inhibitors: Hits and Misses. *J. Med. Chem.* **2018**, *61*, 10976−10995.
(13) Tang, L.; Yang, X.; Liang, Y.; Xie, H.; Dai, Z.; Zheng, G. Transcription Factor Retinoid-Related Orphan Receptor γt: A Promising Target for the Treatment of Psoriasis. *Front. Immunol.* **2018**, *9*, No. 1210.
(14) Sirois, L. E.; Lao, D.; Xu, J.; Angelaud, R.; Tso, J.; Scott, B.; Chakravarty, P.; Malhotra, S.; Gosselin, F. Process Development Overcomes a Challenging Pd-Catalyzed C−N Coupling for the Synthesis of RORc Inhibitor **GDC-0022**. *Org. Process Res. Dev.* **2020**, *24*, 567−578.
(15) Surry, D. S.; Buchwald, S. L. Biaryl Phosphane Ligands in Palladium-Catalyzed Amination. *Angew. Chem., Int. Ed.* **2008**, *47*, 6338−6361.
(16) KOAc as an additive was observed to improve the turnover of the C−N coupling at lower Pd-loadings ≤ 1 mol%, potentially by reversing halogen inhibition via KBr precipitation, and/or by stabilizing catalyst resting state(s).[14]
(17) Kukor, A. J.; St-Jean, F.; Stumpf, A.; Malig, T. C.; Piechowicz, K. A.; Kurita, K.; Hein, J. E. Guided Optimization of a Crystallization-Induced Diastereomer Transformation to Access a Key Navoximod Intermediate. *React. Chem. Eng.* **2023**, *8*, 1294−1299.
(18) Kukor, A. J.; Guy, M. A.; Hawkins, J. M.; Hein, J. E. A Robust New Tool for Online Solution-Phase Sampling of Crystallizations. *React. Chem. Eng.* **2021**, *6*, 2042−2049.
(19) Sato, Y.; Liu, J.; Kukor, A. J.; Culhane, J. C.; Tucker, J. L.; Kucera, D. J.; Cochran, B. M.; Hein, J. E. Real-Time Monitoring of Solid-Liquid Slurries: Optimized Synthesis of Tetrabenazine. *J. Org. Chem.* **2021**, *86*, 14069−14078.
(20) Christensen, M.; Adedeji, F.; Grosser, S.; Zawatzky, K.; Ji, Y.; Liu, J.; Jurica, J. A.; Naber, J. R.; Hein, J. E. Development of an Automated Kinetic Profiling System with Online HPLC for Reaction Optimization. *React. Chem. Eng.* **2019**, *4*, 1555−1558.
(21) Malig, T. C.; Yunker, L. P. E.; Steiner, S.; Hein, J. E. Online High-Performance Liquid Chromatography Analysis of Buchwald−Hartwig Aminations from within an Inert Environment. *ACS Catal.* **2020**, *10*, 13236−13244.
(22) Deem, M. C.; Derasp, J. S.; Malig, T. C.; Legard, K.; Berlinguette, C. P.; Hein, J. E. Ring Walking as a Regioselectivity Control Element in Pd-Catalyzed C-N Cross-Coupling. *Nat. Commun.* **2022**, *13*, No. 2869.
(23) Sharif, S.; Mitchell, D.; Rodriguez, M. J.; Farmer, J. L.; Organ, M. G. *N*-Heteroarylation of Optically Pure α-Amino Esters Using the Pd-PEPPSI-IPentCl-o-Picoline Pre-Catalyst. *Chem. - Eur. J.* **2016**, *22*, 14860−14863.
(24) Ma, X.; Murray, B.; Biscoe, M. R. Stereoselectivity in Pd-Catalysed Cross-Coupling Reactions of Enantioenriched Nucleophiles. *Nat. Rev. Chem.* **2020**, *4*, 584−599.
(25) Wang, C. Y.; Derosa, J.; Biscoe, M. R. Configurationally Stable, Enantioenriched Organometallic Nucleophiles in Stereospecific Pd-Catalyzed Cross-Coupling Reactions: An Alternative Approach to Asymmetric Synthesis. *Chem. Sci.* **2015**, *6*, 5105−5113.
(26) Ballard, A.; Narduolo, S.; Ahmad, H. O.; Cosgrove, D. A.; Leach, A. G.; Buurma, N. J. The Problem of Racemization in Drug Discovery and Tools to Predict It. *Expert Opin. Drug Discovery* **2019**, *14*, 527−539.
(27) Uehling, M. R.; King, R. P.; Krska, S. W.; Cernak, T.; Buchwald, S. L. Organic Chemistry: Pharmaceutical Diversification via Palladium Oxidative Addition Complexes. *Science* **2019**, *363*, 405−408.
(28) (a) Any gaps in data were due to mechanical failure from the sampling probe (no physical change was introduced to the reaction). (b) For simplicity, all heterogeneous component (KOAc, amine **1**, K_3PO_4) concentrations reported in this publication are nominal concentrations based on the initial amount charged. Expanded time course data available in **SI** Section S7.1
(29) He, C.; Ke, J.; Xu, H.; Lei, A. Synergistic Catalysis in the Sonogashira Coupling Reaction: Quantitative Kinetic Investigation of Transmetalation. *Angew. Chem., Int. Ed.* **2013**, *52*, 1527−1530.
(30) Arrechea, P. L.; Buchwald, S. L. Biaryl Phosphine Based Pd(II) Amido Complexes: The Effect of Ligand Structure on Reductive Elimination. *J. Am. Chem. Soc.* **2016**, *138*, 12486−12493.
(31) Ji, Y.; Plata, R. E.; Regens, C. S.; Hay, M.; Schmidt, M.; Razler, T.; Qiu, Y.; Geng, P.; Hsiao, Y.; Rosner, T.; Eastgate, M. D.; Blackmond, D. G. Mono-Oxidation of Bidentate Bis-Phosphines in Catalyst Activation: Kinetic and Mechanistic Studies of a Pd/Xantphos-Catalyzed C−H Functionalization. *J. Am. Chem. Soc.* **2015**, *137*, 13272−13281.
(32) Tereniak, S. J.; Landis, C. R.; Stahl, S. S. Are Phosphines Viable Ligands for Pd-Catalyzed Aerobic Oxidation Reactions? Contrasting Insights from a Survey of Six Reactions. *ACS Catal.* **2018**, *8*, 3708−3714.
(33) Zhang, Y.; Ding, Y.; Pullarkat, S. A.; Li, Y.; Leung, P. H. Chiral Palladacycle Promoted Asymmetric Synthesis of Functionalized Bis-Phosphine Monoxide Ligand. *J. Organomet. Chem.* **2011**, *696*, 709−714.
(34) Chul, W. L.; Jae, S. L.; Nag, S. C.; Kye, D. K.; Sang, M. L.; Jae, S. O. Palladium-Catalyzed Oxidation of Triphenylphosphine. *J. Mol. Catal.* **1993**, *80*, 31−41.
(35) Tanabe, Y.; Nakajima, K.; Nishibayashi, Y. Phosphine Oxidation with Water and Ferrocenium(III) Cation Induced by Visible-Light Irradiation. *Chem. - Eur. J.* **2018**, *24*, 18618−18622.
(36) Tsuneda, T.; Miyake, J.; Miyatake, K. Mechanism of H2O2 Decomposition by Triphenylphosphine Oxide. *ACS Omega* **2018**, *3*, 259−265.
(37) Goering, H. L.; Towns, D. L.; Dittmar, B. Relative Rates of Base-Catalyzed Racemization and Deuterium Exchange of Aryl 2-Octyl Sulfones. *J. Org. Chem.* **1962**, *27*, 736−739.
(38) D'Arrigo, P.; Arosio, D.; Cerioli, L.; Moscatelli, D.; Servi, S.; Viani, F.; Tessaro, D. Base Catalyzed Racemization of Amino Acid Derivatives. *Tetrahedron: Asymmetry* **2011**, *22*, 851−856.
(39) Yuchun, X.; Huizhou, L.; Jiayong, C. Kinetics of Base Catalyzed Racemization of Ibuprofen Enantiomers. *Int. J. Pharm.* **2000**, *196*, 21−26.
(40) Kemp, D. S.; Curran, T. P. Base-Catalyzed Epimerization Behavior and Unusual Reactivity of N-Substituted Derivatives of 2,5-Dicarbalkoxypyrrolidine. Preparation of a Novel Mixed Carbamic Carbonic Anhydride by a 4-(Dimethylamino)Pyridine-Catalyzed Acylation. *J. Org. Chem.* **1988**, *53*, 5729−5731.
(41) Mokhtarzadeh, C. C.; Moore, C. E.; Rheingold, A. L.; Figueroa, J. S. Terminal Iron Carbyne Complexes Derived from Arrested CO_2 Reductive Disproportionation. *Angew. Chem., Int. Ed.* **2017**, *56*, 10894−10899.
(42) Blaschette, A.; Bressel, B. Über Peroxoverbindungen. 3.Mitt. Zur Acidität von Triorganosilylhydroperoxiden [1]. *Inorg. Nucl. Chem. Lett.* **1968**, *4*, 175−178.
(43) Nasielski, J.; Hadei, N.; Achonduh, G.; Kantchev, E. A. B.; O'Brien, C. J.; Lough, A.; Organ, M. G. Structure-Activity Relationship Analysis of Pd-PEPPSI Complexes in Cross-Couplings: A Close Inspection of the Catalytic Cycle and the Precatalyst Activation Model. *Chem. - Eur. J.* **2010**, *16*, 10844−10853.
(44) Relative quantitation by ^{1}H NMR showed slightly more water content in (3*S*,6*R*)-**4** than (3*S*,6*R*)-**2**. For further details see **SI** Table S3
(45) Notably, palladium black was not visibly observable for at least the first 4 h of data acquisition, suggesting that the lack of

https://doi.org/10.1021/acscatal.4c03401
ACS Catal. 2024, 14, 12331−12341

epimerization suppression was not wholly attributable to a limited solution phase concentration of palladium
(46) Kalkman, E. D.; Hartwig, J. F. Direct Observation of Diastereomeric α-C-Bound Enolates during Enantioselective α-Arylations: Synthesis, Characterization, and Reactivity of Arylpalladium Fluorooxindole Complexes. *J. Am. Chem. Soc.* **2021**, *143*, 11741−11750.
(47) A control reaction confirmed that the addition of 1.0 equivalent of water does not impact the outcome of our standard reaction, however the reaction rate was significantly increased (see SI Section S8.2)
(48) Koranne, A.; Kurrey, K.; Kumar, P.; Gupta, S.; Jha, V. K.; Ravi, R.; Sahu, P. K.; Anamika; Jha, A. K. Metal catalyzed C−H functionalization on triazole rings. *RSC Adv.* **2022**, *12*, 27534−27545.
(49) Fuentes-Rivera, J. J.; Zick, M. E.; Düfert, M. A.; Milner, P. J. Overcoming Halide Inhibition of Suzuki-Miyaura Couplings with Biaryl Monophosphine-Based Catalysts. *Org. Process Res. Dev.* **2019**, *23*, 1631−1637.
(50) Carrow, B. P.; Hartwig, J. F. Distinguishing between Pathways for Transmetalation in Suzuki-Miyaura Reactions. *J. Am. Chem. Soc.* **2011**, *133*, 2116−2119.
(51) Wang, C.-Y.; Ralph, G.; Derosa, J.; Biscoe, M. R. Stereospecific Palladium-Catalyzed Acylation of Enantioenriched Alkylcarbastannatranes: A General Alternative to Asymmetric Enolate Reactions. *Angew. Chem., Int. Ed.* **2017**, *56*, 856−860.
(52) Kells, K. W.; Chong, J. M. Stille Coupling of Stereochemically Defined α- Sulfonamidoorganostannanes. *J. Am. Chem. Soc.* **2004**, *126*, 15666−15667.
(53) Ye, J.; Bhatt, R. K.; Falck, J. R. Stereospecific Palladium/Copper Cocatalyzed Cross-Coupling of α-Alkoxy- and α-Aminostannanes with Acyl Chlorides. *J. Am. Chem. Soc.* **1994**, *116*, 1−5.
(54) Lee, B. H.; Choi, Y. L.; Shin, S.; Heo, J. N. Stereoselective Palladium-Catalyzed α-Arylation of 3-Aryl-1-Indanones: An Asymmetric Synthesis of (+)-Pauciflorol F. *J. Org. Chem.* **2011**, *76*, 6611−6618.
(55) Parella, R.; Babu, S. A. Regio- and Stereoselective Pd-Catalyzed Direct Arylation of Unactivated Sp^3 C(3)−H Bonds of Tetrahydrofuran and 1,4-Benzodioxane Systems. *J. Org. Chem.* **2015**, *80*, 2339−2355.
(56) Chen, H.; Deng, M. Z. A Novel Stereocontrolled Synthesis of 1,2-Trans Cyclopropyl Ketones via Suzuki-Type Coupling of Acid Chlorides with Cyclopropylboronic Acids. *Org. Lett.* **2000**, *2*, 1649−1651.
(57) Roh, B.; Farah, A. O.; Kim, B.; Feoktistova, T.; Moeller, F.; Kim, K. D.; Cheong, P. H. Y.; Lee, H. G. Stereospecific Acylative Suzuki-Miyaura Cross-Coupling: General Access to Optically Active α-Aryl Carbonyl Compounds. *J. Am. Chem. Soc.* **2023**, *145*, 7075−7083.
(58) Bordwell, F. G.; Cornforth, F. J. Application of the Hammett Equation to Equilibrium Acidities of Meta-and Para-Substituted Acetophenones. *J. Org. Chem.* **1978**, *43*, 1763−1768.
(59) Bordwell, F. G.; Harrelson, J. A.; Zhang, X. Homolytic Bond Dissociation Energies of Acidic C−H Bonds Activated by One or Two Electron Acceptors. *J. Org. Chem.* **1991**, *56*, 4448−4450.
(60) René, O.; Fauber, B. P.; Malhotra, S.; Yajima, H. Palladium-Catalyzed α-Arylation of Sultams with Aryl and Heteroaryl Iodides. *Org. Lett.* **2014**, *16*, 3468−3471.
(61) He, J.; Wasa, M.; Chan, K. S. L.; Shao, Q.; Yu, J. Q. Palladium-Catalyzed Transformations of Alkyl C−H Bonds. *Chem. Rev.* **2017**, *117*, 8754−8786.

https://doi.org/10.1021/acscatal.4c03401
ACS Catal. 2024, 14, 12331−12341